Contents lists available at ScienceDirect

Digital Chinese Medicine

journal homepage: http://www.keaipublishing.com/dcmed

Modulation of synaptic damage by Bushen Tiansui Decoction via the PI3K signaling pathway in an Alzheimer's disease model

HUI Shan[a], ZHENG Qing[a], LI Hongli[b], ZHU Lemei[b], WU Beibei[b], LIANG Lihui[a*], YANG Jingjing[c*]

a. Department of Geriatrics, Hunan Provincial People's Hospital, The First Affiliated Hospital of Hunan Normal University, Changsha, Hunan 410005, China

b. Department of Integrated Traditional Chinese & Western Medicine, National Clinical Research Center for Metabolic Diseases, The Second Xiangya Hospital, Central South University, Changsha, Hunan 410011, China

c. Teaching and Research Section of Clinical Nursing, National Clinical Research Center for Geriatric Disorders, Xiangya Hospital, Central South University, Changsha, Hunan 410008, China

ARTICLE INFO

Article history
Received 27 July 2024
Accepted 07 September 2024
Available online 25 September 2024

Keywords
Alzheimer's disease (AD)
Synapses
Bushen Tiansui Decoction (补肾填髓方, BSTSD)
Icariin
Phosphoinostitide 3-kinases (PI3K)

ABSTRACT

Objective To explore the therapeutic effect and mechanism of Bushen Tiansui Decoction (补肾填髓方, BSTSD) and its active component icariin on Alzheimer's disease (AD).

Methods (i) Animal experiments. This study conducted experiments using specific pathogen-free (SPF) grade male C57BL/6J wild-type (WT) mice and APP/PS1 double transgenic mice. The animals were divided into three groups: WT group (WT mice, n = 5, receiving distilled water daily), APP/PS1 group (APP/PS1 double transgenic mice, n = 5, receiving distilled water daily), and BSTSD group [APP/PS1 double transgenic mice, n = 5, treated with BSTSD suspension at a dosage of 27 g/(kg·d) for 90 d]. Cognitive function was assessed using the Morris water maze (MWM). Post-experiment, hippocampal tissues were collected for analysis of pyramidal cell and synaptic morphology through hematoxylin-eosin (HE) staining and transmission electron microscopy (TEM). (ii) Cell experiments. The HT-22 cells were divided into control group (untreated), A$\beta_{25\text{-}35}$ group (treated with 20 μmol/L A$\beta_{25\text{-}35}$ for 24 h), icariin group (pre-treated with 20 μmol/L icariin for 60 min, followed by 20 μmol/L A$\beta_{25\text{-}35}$ for an additional 24 h), and icariin + LY294002 group [treated with 20 μmol/L icariin and 20 μmol/L LY294002 (an inhibitor of the phosphoinostitide 3-kinases (PI3K) signaling pathway) for 60 min, then exposed to 20 μmol/L A$\beta_{25\text{-}35}$ for 24 h], and cell viability was measured. Western blot was used to detect the expression levels of synapse-associated proteins [synaptophysin (SYP) and post-synaptic density-95 (PSD-95)] and PI3K signaling pathway associated proteins [phosphorylated (p)-PI3K/PI3K, p-protein kinase B (Akt)/Akt, and p-mechanistic target of rapamycin (mTOR)/mTOR].

Results (i) Animal experiments. Compared with APP/PS1 group, BSTSD group showed that escape latency was significantly shortened (P < 0.01) and the frequency of crossing the original platform was significantly increased (P < 0.01). Morphological observation showed that pyramidal cells in the hippocampal CA1 region were arranged more regularly, nuclear staining was uniform, and vacuole-like changes were reduced after BSTSD treatment. TEM showed that the length of synaptic active zone in BSTSD treatment group was increased compared with APP/PS1 group (P < 0.01), and the width of synaptic gap was decreased (P < 0.01).

*Corresponding author: YANG Jingjing, E-mail: 717441690@qq.com. LIANG Lihui, E-mail: 416284649@qq.com.

Peer review under the responsibility of Hunan University of Chinese Medicine.

DOI: 10.1016/j.dcmed.2024.12.008

Citation: HUI S, ZHENG Q, LI HL, et al. Modulation of synaptic damage by Bushen Tiansui Decoction via the PI3K signaling pathway in an Alzheimer's disease model. Digital Chinese Medicine, 2024, 7(3): 284-293.

(ii) Cell experiments. Icariin had no obvious toxicity to HT-22 cells when the concentration was not more than 20 μmol/L ($P > 0.05$), and alleviated the cell viability decline induced by A$\beta_{25\text{-}35}$ ($P < 0.01$). Western blot results showed that compared with A$\beta_{25\text{-}35}$ group, the ratios of p-PI3K/PI3K, p-Akt/Akt and p-mTOR/mTOR in icariin group were significantly increased ($P < 0.01$), while the protein expression levels of SYP and PSD-95 were increased ($P < 0.01$). These effects were blocked by LY294002 ($P < 0.01$).

Conclusion BSTSD and icariin enhance cognitive function and synaptic integrity in AD models and provide potential therapeutic strategies through activation of the PI3K/Akt/mTOR pathway.

1 Introduction

Alzheimer's disease (AD), a common neurodegenerative disorder, is marked by its insidious onset and progressive deterioration, particularly impairing cognitive functions and memory [1]. Currently, approximately 55 million individuals worldwide are affected by AD, with projections estimating over 150 million cases by 2050, highlighting its significant burden on global health [2, 3]. Pathologically, AD is characterized by amyloid-β (Aβ) deposition, leading to the formation of amyloid plaques, and tau protein aggregation, resulting in neurofibrillary tangles [4]. Synaptic dysfunction, manifested as synaptic loss, damage, and structural changes, often precedes the onset of behavioral symptoms in the early stages of AD [5, 6]. Identifying the mechanisms behind synaptic impairment and developing synapse-targeted therapies could provide more effective treatment strategies and improve patient outcomes. However, current pharmacological treatments yield only limited benefits in decelerating cognitive decline and alleviating behavioral symptoms [7], underscoring the pressing need for innovative therapeutic approaches to effectively manage AD.

Bushen Tiansui Decoction (补肾填髓方, BSTSD), also known as Naoling Decoction, is a widely utilized herbal remedy in traditional Chinese medicine (TCM). It consists of six primary components: Yinyanghuo (Epimedii Folium), Heshouwu (Polygoni Multiflori Radix), Guiban (Carapax Testudinis), Longgu (Os Draconis), Shichangpu (Acori Tatarinowii Rhizoma), and Yuanzhi (Polygalae Radix) [8, 9]. Yinyanghuo (Epimedii Folium) and Heshouwu (Polygoni Multiflori Radix), renowned for their anti-dementia properties, serve as the principal ingredients, while Guiban (Carapax Testudinis) and Longgu (Os Draconis), which enhance essence and nourish marrow, act as supplementary agents. Shichangpu (Acori Tatarinowii Rhizoma) and Yuanzhi (Polygalae Radix), known for regulating the functions of the nine orifices, provide additional support. In prior research, BSTSD's composition was qualitatively analyzed using ultrahigh-performance liquid chromatography-tandem mass spectrometry (UPLC-MS), identifying icariin as a key active component in the formula [10]. Previous studies evaluated the effects of three different BSTSD doses [9, 27, and 54 g/(kg·d)] on memory and learning in AD models, with the 27 g/(kg·d) dose demonstrating the best therapeutic outcomes and minimal side effects, making it the preferred dosage for further studies [9, 11]. Moreover, our previous findings have highlighted icariin's capacity to mitigate Aβ toxicity and enhance cognitive function [12]. Nonetheless, the underlying mechanisms driving BSTSD and icariin's beneficial effects in AD therapy remain poorly understood, requiring deeper investigation.

Cognitive decline in AD has been strongly associated with synaptic loss and impairments [13]. The soluble Aβ oligomers have been shown to induce synaptic loss through the phosphoinostitide 3-kinase (PI3K)/protein kinase B (Akt) signaling pathway, thereby impairing synaptic structure and function [14]. A comprehensive investigation integrating network pharmacology and serum metabolomics identified the PI3K/Akt pathway as a possible mechanism for BSTSD's cognitive benefits in AD [15]. The mechanistic target of rapamycin (mTOR), a key regulator of cellular growth and proliferation, interacts with the PI3K/Akt/mTOR signaling pathway to mediate processes such as cell survival and metabolism. Presynaptic proteins like synaptophysin (SYP) and postsynaptic proteins such as postsynaptic density-95 (PSD-95) are integral to synaptic plasticity and cognitive function [7]. Yet, the specific interactions between BSTSD, synaptic plasticity-related proteins, and the PI3K signaling pathway in the context of AD remain unclear and merit further study.

Therefore, this study aimed to evaluate the potential of BSTSD in improving memory and cognition using APP/PS1 mice, a transgenic model of AD, and explore the molecular mechanisms of icariin within an AD cellular framework (HT-22 cells).

2 Materials and methods

2.1 Reagents and instruments

We used the following reagents in this study: Milk powder (Biosharp, China); icariin powder (Nanjing Spring & Autumn Biological Engineering Co., Ltd., China); sodium pentobarbital (Sigma-Aldrich, USA); transmission

electron microscopy (TEM) fixative (Agar Scientific, UK); Dulbecco's modified Eagle medium (DMEM) (Gibco, USA); fetal bovine serum (FBS) (Gibco, USA); A$\beta_{25\text{-}35}$ (MedChemExpress, USA); dimethyl sulfoxide (DMSO) (Sinopharm Chemical Reagent, China); LY294002 (APExBIO, USA); 4% paraformaldehyde, bovine serum albumin (BSA), cell-counting kit-8 assay kit (CCK-8), radio immunoprecipitation assay (RIPA) lysis buffer, and bicinchoninic acid (BCA) protein assay kit (Beyotime Biotechnology, China); 10% sodium dodecyl sulfate-polyacrylamide gel electrophoresis (SDS-PAGE) (Bio-Rad, USA); polyvinylidene difluoride (PVDF) membranes (Millipore-Sigma, USA); PI3K antibody, p-PI3K antibody, p-Akt antibody, Akt antibody, mTOR antibody and p-mTOR antibody (Cell Signaling Technology, USA); PSD-95 antibody, SYP antibody and β-actin antibody (ProteinTech, USA); goat anti-mouse secondary antibody and goat anti-rabbit secondary antibody (Abiowell, China); and enhanced chemiluminescence (ECL) solution (Thermo Fisher Scientific, USA).

Instruments used including transmission electron microscope (Hitachi, HT7800); camera (Canon, XF605); light microscope (Leica, DM1000); microplate reader (BioTek, Synergy LX); gel documentation system (Guangzhou Biolight Biotechnology Co., Ltd., Gelview 6000 Pro); morris water maze (MWM) (Xinruan Information Technology Co., Ltd., XR-XM101); superclean bench (Thermo Fisher Scientific, HeraSafe 202); high-speed refrigerated centrifuge (Beckman Coulter, Avanti J-26S).

2.2 BSTSD preparation

The BSTSD extract, composed of six herbs, Yinyanghuo (Epimedii Folium), Heshouwu (Polygoni Multiflori Radix), Guiban (Carapax Testudinis), Longgu (Os Draconis), Shichangpu (Acori Tatarinowii Rhizoma), and Yuanzhi (Polygalae Radix), is mixed in a 3 : 3 : 4 : 4 : 2 : 2 ratio, respectively. The extracts were sourced from Tongrentang Pharmaceutical Co., Ltd. (Beijing, China) [9, 10], with plant names verifiable through http://mpns.kew.org. Voucher specimens (No. TCM20200369) were archived at the Second Xiangya Hospital of Central South University [8]. Stringent quality control protocols were applied during extraction. The process involved treating the herbal mixture with distilled water, followed by boiling and filtration. Initially, a 10 : 1 water-to-medicine ratio was employed, and reduced to 8 : 1 in a subsequent decoction. The filtrate was then concentrated and dried using a vacuum freeze-dryer. To maintain BSTSD's quality, chromatographic fingerprinting was conducted via UPLC-MS, focusing on the primary components. Standard compounds (purity > 98%) were obtained from the National Standard Center, and a CNW Athena C18-WP column was utilized at 35 °C with gradient elution. The mobile phase consisted of water and CH_3CN, and icariin was identified as a major component, detected at 270 nm with a flow rate of 0.5 mL/min [10].

2.3 Animals grouping and treatment

Specific pathogen-free (SPF) grade male 6-month-old APP/PS1 double transgenic (n = 10) and C57BL/6J WT mice (n = 5) were utilized, with a weight range of 25 – 35 g. The mice were purchased from Sibeifu (Beijing) Biotechnology Co., Ltd. [experimental animal license number: SCXK (Jing) 2019-0010], with facility license number SYXK (Xiang) 2017-0003. All mice were maintained under SPF conditions, housed in a controlled environment with a 12 h light-dark cycle, a temperature of 24 – 26 °C, relative humidity of 40% – 60%, minimal noise, and unrestricted access to food and water [12]. The study protocols adhered to the ethical standards set by the Institutional Animal Ethics Committee of Hunan Normal University, China, with the relevant approval (2021-047). Prior research evaluated the efficacy of BSTSD at three distinct dosages [9, 27, and 54 g/(kg·d)]. Results demonstrated that the 27 g/(kg·d) dose provided optimal efficacy while minimizing adverse effects [9, 11]. Based on these data, this dosage was chosen for subsequent experiments. Prior to treatment, BSTSD powder was prepared by dissolving it in distilled water to create a suspension at a concentration of 27 g/(kg·d). This suspension was prepared fresh before each administration to ensure optimal efficacy. The mice were divided into WT group (WT mice, n = 5, receiving distilled water daily), APP/PS1 group (APP/PS1 double transgenic mice, n = 5, receiving distilled water daily), and BSTSD group [APP/PS1 double transgenic mice, n = 5, treated with BSTSD suspension at a dosage of 27 g/(kg·d) for 90 d].

2.4 MWM test

A circular stainless steel tank, with a diameter of 120 cm and a height of 45 cm, was employed for the MWM experiment. The tank was filled with water to a depth of 25 cm, and the water temperature was maintained at 22 ± 2 °C throughout the experiment to prevent any impact on the mice due to temperature fluctuations. To enhance visibility, milk powder was added to the water, creating a white surface, as the mice with dark fur could obscure visibility. A cylindrical platform, with a diameter of 12 cm and a height of 24 cm, was positioned in the center of one quadrant. During the 5 d navigation trial period, each mouse was introduced vertically into the water, consistently oriented toward the pool wall, with each session lasting 60 s. On the 6th day, the platform was removed to conduct the spatial probe test, and the number of times the mice crossed the area corresponding to the former location of the hidden platform within 60 s was recorded, following previously described methods [9]. Swimming trajectories

were recorded using an overhead camera, and data analysis, including trajectory mapping, was performed with Smart 3.0 software.

2.5 TEM

Mice were anesthetized with sodium pentobarbital administered by intraperitoneal injection at a dose of 30 – 60 mg/kg. Following anesthesia, cervical dislocation was performed to euthanize the mice. The brains were quickly removed on ice, and a 1 mm^3 hippocampal tissue sample containing the CA1 region was transferred to an Eppendorf (EP) tube containing fresh TEM fixative and preserved at 4 °C. Post-fixation, the sample was immersed in 1% OsO_4 solution in 0.1 mol/L phosphate buffer (pH 7.4) for 2 h under dark conditions [16]. The tissue was then dehydrated through graded ethanol series and embedded in resin. Ultrathin sections (60 – 80 nm) were cut from the resin-embedded tissues and placed onto 150-mesh copper grids coated with formvar film. The sections were stained with 2% uranyl acetate for 10 min, followed by a 5 min lead citrate treatment. Imaging was performed using a transmission electron microscope, and the resulting images were collected for subsequent analysis.

2.6 Hematoxylin-eosin (HE) staining

Mice were anesthetized with sodium pentobarbital via intraperitoneal injection at a dose of 30 – 60 mg/kg, after which cervical dislocation was performed to euthanize them. Following euthanasia, the brains were quickly removed and rinsed in pre-cooled phosphate-buffered saline (PBS) to clean the tissue. The brain tissue was then fixed in 4% paraformaldehyde for at least 24 h. After fixation, the brain tissue was subjected to graded ethanol dehydration (75%, 85%, 95%, and 100%) [17], followed by immersion in three successive xylene baths (I, II, and III) for 20 min each. The tissue was then infiltrated with wax (I and II) for 60 min and sectioned coronally at a thickness of 4 μm using a microtome. After staining with hematoxylin for 5 min, the slides were rinsed with water to remove excess stain. A 30 s treatment with 1% hydrochloric acid in alcohol was applied, followed by color restoration using 0.6% ammonia. A subsequent water rinse preceded a 2-min eosin staining. Final dehydration with ethanol and xylene was performed, and the sections were sealed with neutral resin. After allowing them to dry naturally, the sections were placed under a light microscope for observation.

2.7 Cell culture

HT-22 mouse hippocampal neuronal cells (Wuhan Sunncell, SNL-202, China) were derived from mouse hippocampal tissue. They were cultured in DMEM supplemented with 10% fetal bovine serum and 1% penicillin/streptomycin (P/S) under standard conditions of 5% CO_2 at 37 °C. Cells were passaged every 1 – 2 d depending on their confluence, and consistently subcultured 2 – 3 times prior to experimental use. A$\beta_{25\text{-}35}$ is known for its neurotoxic effects and is commonly used to induce cell injury *in vitro* models of AD. Icariin powder (⩾ 98% purity) was dissolved in DMSO [12]. LY294002 is a PI3K inhibitor to block the activity of the PI3K signaling pathway. For experimentation, cells were plated in six-well plates at a density of 10^5 cells/mL and assigned to control group (untreated), A$\beta_{25\text{-}35}$ group (treated with 20 μmol/L A$\beta_{25\text{-}35}$ for 24 h), icariin group (pre-treated with 20 μmol/L icariin for 60 min, followed by 20 μmol/L A$\beta_{25\text{-}35}$ for an additional 24 h), and icariin + LY294002 group [treated with 20 μmol/L icariin and 20 μmol/L LY294002 [18] for 60 min, then exposed to 20 μmol/L A$\beta_{25\text{-}35}$ for 24 h].

2.8 Cell viability assay

The cell viability of HT-22 cells was evaluated using the CCK-8 assay [19]. HT-22 cells were seeded in 96-well plates at a density of 1 × 10^5 cells/mL. After 24 h of exposure to A$\beta_{25\text{-}35}$ (0, 5, 10, 20, and 40 μmol/L) or icariin (0, 5, 10, 20, and 40 μmol/L), CCK-8 solution was introduced into each well. The plates were incubated for 1 h, after which absorbance at 450 nm was measured using a microplate reader. Cell viability was calculated as the percentage of absorbance at 450 nm compared with the vehicle control. Each experiment included a blank control, with five parallel replicates and repeated three times to ensure reproducibility.

2.9 Western blot assay

Western blot analysis was performed as described previously [8]. Total proteins were extracted using cold RIPA lysis buffer supplemented with protease and phosphatase inhibitors. Protein concentration was determined using the BCA assay. Equal amounts of protein samples were loaded and separated by 10% SDS-PAGE. Following electrophoresis, the samples were transferred to PVDF membranes and blocked with 1% BSA. The membranes were incubated overnight at 4 °C with the respective primary antibodies, including PI3K (1 : 1 000), p-PI3K (1 : 1 000), p-Akt (1 : 1 000), Akt (1 : 2 000), mTOR (1 : 1 000), p-mTOR (1 : 1 000), PSD-95 (1 : 5 000), SYP (1 : 5 000), and β-actin (1 : 5 000). After three washes with TBST (0.1% Tween 20 in Tris-HCl buffer), the membranes were incubated with goat anti-mouse (1 : 5 000) or anti-rabbit (1 : 5 000) secondary antibodies for 90 min. Chemiluminescent detection was performed using ECL solution, with excess reagent removed by blotting before wrapping the membranes in plastic for imaging with a gel documentation system. Band intensities were quantified using ImageJ software.

2.10 Statistical analysis

The data were represented as mean ± standard deviation (SD) and analyzed using SPSS 27.0. A repeated-measures analysis of variance (ANOVA) was applied to assess escape latency, while intergroup differences were evaluated through one-way ANOVA with subsequent least significant difference (LSD) post hoc testing. $P < 0.05$ was considered statistically significant.

3 Results

3.1 Alleviation of memory decline by BSTSD in APP/PS1 mice

The MWM test was utilized to assess spatial learning and memory. Trajectories recorded over the 5 d navigation task were analyzed for cognitive function evaluation (Figure 1A). On the 6th day, a probe trial measured spatial memory retention within 60 s across different groups (Figure 1B). During the navigation experiment, escape latency (the time taken to locate the hidden platform) was recorded over five consecutive days. The APP/PS1 group exhibited a significantly longer escape latency compared with the WT group ($P < 0.01$, Figure 1C). BSTSD treatment resulted in a significant reduction in escape latency compared with APP/PS1 group ($P < 0.01$) (Figure 1C). In the probe trial, the number of crossings (the frequency of traversing the original platform location after its removal) was recorded. APP/PS1 group showed a significantly reduced number of crossings compared with WT group ($P < 0.01$, Figure 1D). In contrast, BSTSD treatment significantly increased the number of crossings in APP/PS1 mice ($P < 0.01$). These findings indicate that BSTSD treatment improves spatial learning and memory retention in an AD model.

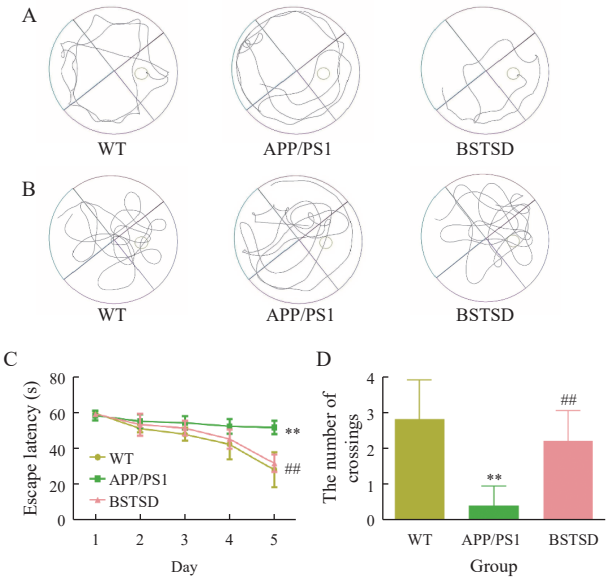

Figure 1 Effects of BSTSD on spatial learning and memory deficits in APP/PS1 mice in MWM test ($n = 5$)

A, representative swim trajectories on day 5 of the navigation training. B, representative swim trajectories during the probe trial. C, escape latency. D, the number of crossings. Data were represented as mean ± SD. $^{**}P < 0.01$, compared with WT group. $^{\#\#}P < 0.01$, compared with APP/PS1 group.

3.2 Mitigation of pyramidal cell and synaptic ultrastructural degradation by BSTSD in APP/PS1 mice

In WT mice, pyramidal cells in the CA1 region of the hippocampus exhibited a normal orientation and typical histological characteristics. In contrast, APP/PS1 mice displayed disorganized neuronal arrangements, along with darkly stained, vacuolated nuclei. Following 90 d of BSTSD treatment, the APP/PS1 mice showed improved cellular organization and a reduction in darkly stained, vacuolated nuclei (Figure 2A), indicating that BSTSD treatment alleviates histopathological alterations associated with AD.

To assess the impact of BSTSD on synaptic ultrastructure, TEM analysis was performed. APP/PS1 mice, compared with WT, demonstrated hippocampal synaptic swelling, a reduction in synaptic vesicles (Figure 2B), decreased synaptic active zone (SAZ) ($P < 0.01$, Figure 2C), and widening of the synaptic cleft ($P < 0.01$, Figure 2D). In contrast, BSTSD group exhibited a more preserved synaptic architecture, with increased SAZ length ($P < 0.01$, Figure 2C) and a narrower synaptic cleft compared with APP/PS1 group ($P < 0.01$, Figure 2D).

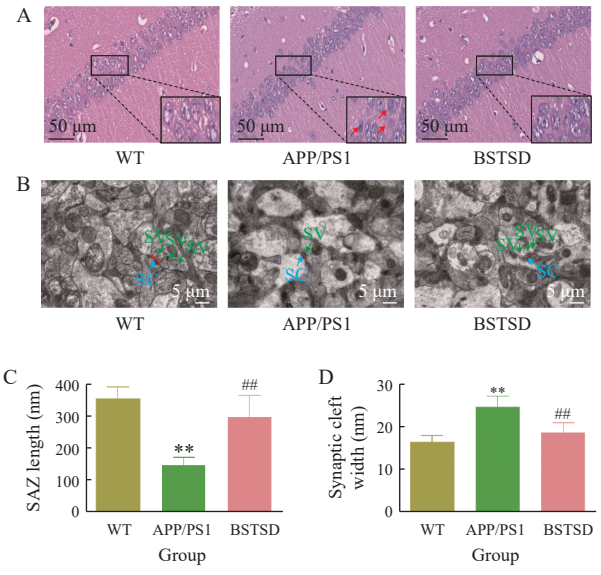

Figure 2 Neuroprotective effects of BSTSD in the hippocampus ($n = 5$)

A, representative HE-stained images of the hippocampus, with red arrows highlighting pyramidal cells displaying irregular neuronal arrangement, intensely stained, and vacuolated nuclei. B, representative TEM images of hippocampal synaptic structures (10 000 ×). Red lines mark the SAZ. C, quantitative analysis of SAZ length in hippocampal synapses. D, quantitative analysis of synaptic cleft width. Data were represented as mean ± SD. $^{**}P < 0.01$, compared with WT group. $^{\#\#}P < 0.01$, compared with APP/PS1 group.

3.3 Effects of icariin and A$\beta_{25\text{-}35}$ on HT-22 cell viability

Icariin has no toxic effect on HT22 cells at concentrations up to 20 μmol/L for 24 h ($P > 0.05$), but at a concentration of 40 μmol/L, cell viability is significantly reduced ($P < 0.01$, Figure 3A). In contrast, A$\beta_{25\text{-}35}$ exposure at 20 μmol/L or higher significantly impaired HT-22 cell viability ($P < 0.01$, Figure 3B). Icariin demonstrated a protective role, mitigating the cytotoxic effects induced by A$\beta_{25\text{-}35}$ in HT-22 cells ($P < 0.01$, Figure 3C). Additionally, A$\beta_{25\text{-}35}$ treatment inhibited HT-22 cell proliferation, whereas icariin administration restored cell viability, with a notable improvement ($P < 0.01$).

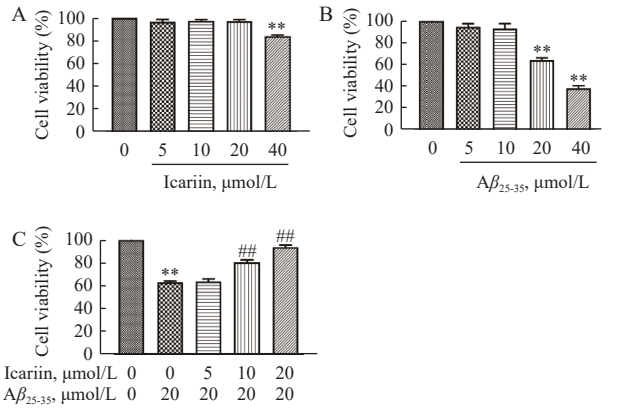

Figure 3 Effects of varying concentrations of icariin and A$\beta_{25\text{-}35}$ in HT-22 cells ($n = 5$)

A, cell viability of HT-22 cells treated with icariin. B, cell viability of HT-22 cells treated with A$\beta_{25\text{-}35}$. C, the protective effects of icariin against A$\beta_{25\text{-}35}$-induced cytotoxicity in HT-22 cells. Data were represented as mean ± SD. $^{**}P < 0.01$, compared with 0 μmol/L group. $^{\#\#}P < 0.01$, compared with A$\beta_{25\text{-}35}$ (20 μmol/L) + icariin (0 μmol/L) group.

3.4 Regulation of the PI3K/Akt/mTOR pathway by icariin in HT-22 cells

The study revealed significant decreases in the p-PI3K/PI3K, p-Akt/Akt, and p-mTOR/mTOR ratios in A$\beta_{25\text{-}35}$ group compared with control group ($P < 0.01$), confirming the involvement of the PI3K/Akt/mTOR signaling pathway in A$\beta_{25\text{-}35}$-induced effects on HT-22 cells. Notably, icariin treatment led to a marked increase in the expression levels of these ratios in the HT-22 cells ($P < 0.01$). However, co-treatment with LY294002 effectively nullified icariin's protective effects ($P < 0.01$), further corroborating the role of the PI3K/Akt/mTOR pathway in icariin-mediated protection of HT-22 cells (Figure 4).

3.5 Enhancement of PI3K/Akt/mTOR-mediated synapse-associated protein expression by icariin in A$\beta_{25\text{-}35}$-stimulated HT-22 cells

Icariin upregulated synapse-associated protein expression through the PI3K/Akt/mTOR pathway in A$\beta_{25\text{-}35}$-

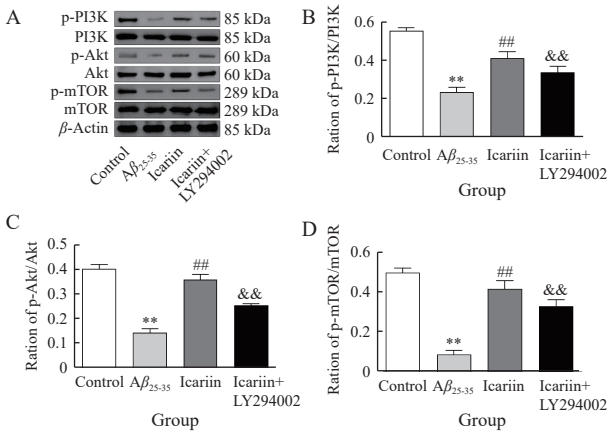

Figure 4 Effects of icariin on the PI3K/Akt/mTOR signaling pathway ($n = 3$)

A, Western blot images of phosphorylated and total PI3K, Akt, mTOR, and β-actin proteins. B – D, ratios of the p-PI3K/PI3K, p-Akt/Akt, and p-mTOR/mTOR ratios, respectively. Data were represented as mean ± SD. $^{**}P < 0.01$, compared with control group. $^{\#\#}P < 0.01$, compared with A$\beta_{25\text{-}35}$ group. $^{\&\&}P < 0.01$, compared with icariin group.

stimulated HT-22 cells. Although A$\beta_{25\text{-}35}$ caused a reduction in SYP and PSD-95 protein levels ($P < 0.01$), pretreatment with icariin effectively prevented this decline ($P < 0.01$). Furthermore, the protective role of icariin was negated by LY294002 ($P < 0.01$, Figure 5).

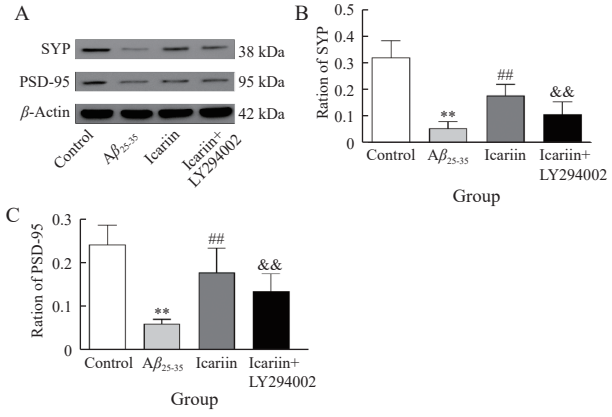

Figure 5 Effects of icariinon synaptic proteins damaged by A$\beta_{25\text{-}35}$ in HT-22 cells ($n = 3$)

A, Western blot images of SYP and PSD-95 proteins. B and C, ratios of SYP and PSD-95, respectively. Data were represented as mean ± SD. $^{**}P < 0.01$, compared with control group. $^{\#\#}P < 0.01$, compared with A$\beta_{25\text{-}35}$ group. $^{\&\&}P < 0.01$, compared with icariin group.

4 Discussion

TCM provides distinctive therapeutic benefits for treating AD. Among these, BSTSD has demonstrated potential anti-dementia effects [10]. However, the specific mechanisms of action remain largely unexplored. This study employed the MWM test to assess the impact of BSTSD on spatial learning and memory impairments. The results indicated a significant enhancement in spatial cognition

in APP/PS1 mice following BSTSD administration, underscoring its potential as an effective TCM treatment for AD. The current findings contribute novel insights into the effects of BSTSD on spatial learning and memory impairments in AD models. Icariin, the principal active component of Yinyanghuo (Epimedii Folium), is considered a promising therapeutic agent for neurological disorders. Icariin has been shown to inhibit phosphodiesterase-5 activity and mitigate the formation of both intracellular and extracellular neurofibrillary tangles [20]. The current findings also support the neuroprotective role of icariin, highlighting its potential as a multitarget therapeutic agent for slowing AD progression [21, 22]. Study has identified icariin as the main bioactive compound in BSTSD that reaches the brain [10]. This research aims to establish experimental and theoretical foundations for the anti-dementia efficacy of BSTSD and to explore the mechanisms by which BSTSD exerts neuroprotective effects against synaptic damage and memory impairment, particularly focusing on the mechanisms of action of icariin.

Synaptic loss is a hallmark of the early stages of AD and is closely linked to cognitive decline. A key player in the pathological mechanisms underlying AD is Aβ, particularly through its interactions with neuronal synapses. Research has demonstrated that soluble Aβ oligomers bind to synaptic proteins, leading to synaptic dysfunction and degeneration [23]. This process is critical, as the redistribution of these key synaptic proteins in response to Aβ binding contributes significantly to synaptic impairment. Targeting toxic Aβ or disrupted synaptic pathways represents a promising early intervention strategy that may halt or even reverse the progression of AD [24]. The impact of soluble Aβ oligomers on synaptic proteins further emphasizes the importance of addressing these pathological changes, as this redistribution is a key factor in synaptic dysfunction and degeneration [25]. The present study shows that BSTSD treatment, demonstrated in APP/PS1 mice significantly enhances synaptic structure. Notable observations in BSTSD group included elongated synaptic vesicles, an enlarged SAZ, and a reduced synaptic cleft width compared with controls. Additionally, pyramidal cells in BSTSD group displayed improved structural integrity, evidenced by enhanced organization, intensified staining, and diminished nuclear vacuolization, as revealed by HE staining. These findings suggest that BSTSD mitigates synaptic damage and may exert anti-dementia effects by modulating synaptic architecture. Key synaptic proteins, such as SYP and PSD-95, play crucial roles in regulating hippocampal synaptic plasticity, directly impacting cognitive function and memory. PSD-95, in particular, binds to the C-terminal domain (CTD) of N-methyl-D-aspartate (NMDA) receptors, thereby modulating synaptic plasticity and neurotransmission. In AD transgenic models, Aβ oligomers have been observed to co-localize with PSD-95 at postsynaptic terminals, indicating significant alterations in synaptic structure and function [26]. Furthermore, Aβ has been shown to reduce endogenous PSD-95 levels in the NMDA receptor CTD, exacerbating synaptic dysfunction [26]. Synaptic dysfunction, along with decreased expression levels of SYP and PSD-95 and the loss of hippocampal neurons, has also been associated with tau hyperphosphorylation in rat models [27]. Notably, both SYP and PSD-95, critical markers of synaptic density, show significant reductions preceding amyloid plaque formation in AD mouse models [28, 29]. These insights underline the pivotal role of Aβ in synaptic pathology and highlight the potential of targeting Aβ-mediated synaptic alterations for the development of therapeutic strategies for AD.

The PI3K/Akt signaling pathway is integral to various cellular functions, including survival, growth, differentiation, motility, intracellular transport, and neurite outgrowth [30, 31]. It also modulates neurotransmission and synaptic plasticity [31]. PI3K/Akt expression has been found to be reduced in AD brain tissue [32]. mTOR, which intersects with the PI3K/Akt pathway, is involved in four major signaling cascades and plays a key role in central nervous system function [33]. Study suggests that upregulation of PI3K/Akt/mTOR signaling can elevate synaptic protein levels in the prefrontal cortex, thereby strengthening synaptic connections via related mechanisms [34]. Similarly, enhancement of this pathway may facilitate synaptic protein synthesis and myelin protein expression, contributing to neuroprotection [35, 36]. Targeting the PI3K/Akt/mTOR signaling pathway, therefore, presents a promising therapeutic approach for addressing neurodegenerative diseases like AD. In the context of an AD cellular model using HT-22 cells, exposure to A$\beta_{25\text{-}35}$ resulted in a significant reduction in key synaptic proteins, including SYP and PSD-95. Additionally, there was a notable decrease in the ratios of phosphorylated PI3K (p-PI3K), Akt (p-Akt), and mTOR (p-mTOR) compared with their respective total protein levels. This indicates a disruption in the signaling pathways crucial for synaptic integrity and function, further implicating A$\beta_{25\text{-}35}$ in the pathophysiology of AD. To further elucidate the involvement of the PI3K/Akt/mTOR signaling pathway in synaptic damage induced by A$\beta_{25\text{-}35}$, the PI3K inhibitor LY294002 was used in the present study. Icariin treatment was found to effectively restore levels of synaptic proteins and the ratios of phosphorylated PI3K, Akt, and mTOR to their total protein levels, highlighting its therapeutic potential in reversing synaptic impairment. However, the PI3K inhibitor LY294002 inhibited the PI3K/Akt/mTOR signaling pathway and concomitantly reduced the expression levels of synaptic proteins. After the addition of the PI3K pathway inhibitor LY294002, the effect of icariin was attenuated

but not completely abolished, indicating that icariin primarily regulates synaptic function through the PI3K pathway. However, this is not the sole pathway involved, which aligns with the evolutionary concept of a networked regulatory mode where multiple pathways converge to regulate a single phenotype. These findings suggest that future research should explore additional pathways involved in icariin's neuroprotective effects and investigate potential synergistic interactions with the PI3K pathway. A deeper understanding of these network interactions could lead to more targeted therapeutic strategies for neuroprotection.

This research highlights the innovative potential of BSTSD and its active component, icariin, in managing AD by modulating synaptic architecture and the PI3K/Akt/mTOR signaling pathway. These findings introduce a novel therapeutic approach to AD through TCM. However, several limitations should be acknowledged. While this study demonstrates the therapeutic effects of BSTSD and icariin on memory deficits and synaptic damage, further investigation is needed to explore the mechanisms of BSTSD *in vitro* to more clearly delineate its neuroprotective effects. Moreover, although icariin exhibited protective effects in HT-22 cells, its mechanisms *in vivo* within APP/PS1 mice require further exploration to understand its interactions with biological pathways and to assess its therapeutic potential. While this study offers promising insights into the neuroprotective effects of BSTSD and icariin, more comprehensive research is essential to fully elucidate the underlying mechanisms and establish their clinical relevance. Future studies should aim to expand the investigation of TCM-based approaches for neurodegenerative disease therapies, potentially integrating BSTSD and icariin into broader treatment paradigms.

5 Conclusion

This study demonstrated therapeutic potential of BSTSD in alleviating memory deficits associated with AD. Additionally, icariin demonstrated synaptic protection in HT-22 cells by activating the PI3K/Akt/mTOR signaling pathway. Although the precise molecular targets of BSTSD and icariin remain unidentified, these findings offer valuable insights into the mechanisms underlying their neuroprotective effects against cognitive decline, lays a strong foundation for further investigations into the integration of TCM into therapeutic strategies for AD, and enhance both theoretical understanding and practical application.

Fundings

Hunan Provincial Natural Science Foundation of China (2022JJ40220), Health Commission of Hunan Province (B202303106781), and Hunan Administration of Traditional Chinese Medicine (2021192).

Competing interests

The authors declare no conflict of interest.

References

[1] LOURENCO MV, FROZZA RL, DE FREITAS GB, et al. Exercise-linked FNDC5/irisin rescues synaptic plasticity and memory defects in Alzheimer's models. Nature Medicine, 2019, 25(1): 165–175.

[2] 2023 Alzheimer's disease facts and figures. Alzheimers Dementia, 2023, 19(4): 1598-1695.

[3] NICHOLS E, STEINMETZ JD, VOLLSET SE, et al. Estimation of the global prevalence of dementia in 2019 and forecasted prevalence in 2050: an analysis for the Global Burden of Disease Study 2019. The Lancet Public Health, 2022, 7(2): e105–e125.

[4] DUBOIS B, VILLAIN N, FRISONI GB, et al. Clinical diagnosis of Alzheimer's disease: recommendations of the International Working Group. The Lancet Neurology, 2021, 20(6): 484–496.

[5] PENG L, BESTARD-LORIGADOS I, SONG WH. The synapse as a treatment avenue for Alzheimer's disease. Molecular Psychiatry, 2022, 27(7): 2940–2949.

[6] JOHN A, REDDY PH. Synaptic basis of Alzheimer's disease: focus on synaptic amyloid beta, P-tau and mitochondria. Ageing Research Reviews, 2021, 65: 101208.

[7] TZIORAS M, MCGEACHAN RI, DURRANT CS, et al. Synaptic degeneration in Alzheimer disease. Nature Reviews Neurology, 2023, 19(1): 19–38.

[8] LI HL, TAN YJ, CHENG X, et al. Untargeted metabolomics analysis of the hippocampus and cerebral cortex identified the neuroprotective mechanisms of Bushen Tiansui formula in an A$\beta_{25\text{-}35}$-induced rat model of Alzheimer's disease. Frontiers in Pharmacology, 2022, 13: 990307.

[9] WANG Z, HUI S, YANG Y, et al. Protective effects of Bushen Tiansui decoction on hippocampal synapses in a rat model of Alzheimer's disease. Neural Regeneration Research, 2017, 12(10): 1680.

[10] SHENG CX, XU PP, LIU XY, et al. Bushen-Tiansui Formula improves cognitive functions in an A$\beta_{1\text{-}42}$ fibril-infused rat model of Alzheimer's disease. Neural Plasticity, 2020, 2020: 1–11.

[11] XIA ZA, PENG WJ, CHENG SH, et al. Naoling decoction restores cognitive function by inhibiting the neuroinflammatory network in a rat model of Alzheimer's disease. Oncotarget, 2017, 8(26): 42648–42663.

[12] LIU YQ, LI HL, WANG XW, et al. Anti-Alzheimers molecular mechanism of icariin: insights from gut microbiota, metabolomics, and network pharmacology. Journal of Translational Medicine, 2023, 21(1): 277.

[13] JU YJ, TAM KY. Pathological mechanisms and therapeutic strategies for Alzheimer's disease. Neural Regeneration Research, 2022, 17(3): 543.

[14] BAEK H, SANJAY, PARK M, et al. Cyanidin-3-*O*-glucoside protects the brain and improves cognitive function in APPswe/PS1ΔE9 transgenic mice model. Journal of Neuroinflammation, 2023, 20(1): 268.

[15] ZHANG ZY, YI PJ, YANG JJ, et al. Integrated network pharmacology analysis and serum metabolomics to reveal the

cognitive improvement effect of Bushen Tiansui formula on Alzheimer's disease. Journal of Ethnopharmacology, 2020, 249: 112371.

[16] CAI MD, LEE JH, YANG EJ. Electroacupuncture attenuates cognition impairment via anti-neuroinflammation in an Alzheimer's disease animal model. Journal of Neuroinflammation, 2019, 16(1): 264.

[17] FU PF, BAI LR, CAI ZW, et al. Fine particulate matter aggravates intestinal and brain injury and affects bacterial community structure of intestine and feces in Alzheimer's disease transgenic mice. Ecotoxicology and Environmental Safety, 2020, 192: 110325.

[18] HUANG AM, ZENG PT, LI YG, et al. LY294002 is a promising inhibitor to overcome sorafenib resistance in FLT3-ITD mutant AML cells by interfering with PI3K/Akt signaling pathway. Frontiers in Oncology, 2021, 11: 782065.

[19] YANG SX, XIE ZP, PEI TT, et al. Salidroside attenuates neuronal ferroptosis by activating the Nrf2/HO1 signaling pathway in A$\beta_{1\text{-}42}$-induced Alzheimer's disease mice and glutamate-injured HT22 cells. Chinese Medicine, 2022, 17(1): 82.

[20] ANGELONI C, BARBALACE MC, HRELIA S. Icariin and its metabolites as potential protective phytochemicals against Alzheimer's disease. Frontiers in Pharmacology, 2019, 10: 271.

[21] LIU J, WEI AH, LIU TT, et al. Icariin ameliorates glycolytic dysfunction in Alzheimer's disease models by activating the Wnt/β-catenin signaling pathway. The FEBS Journal, 2024, 291(10): 2221–2241.

[22] WU BB, XIAO Q, ZHU LM, et al. Icariin targets p53 to protect against ceramide-induced neuronal senescence: implication in Alzheimer's disease. Free Radical Biology Medicine, 2024, 224: 204–219.

[23] NAKAMURA M, LI YH, CHOI BR, et al. GDE2-RECK controls ADAM10 alpha-secretase-mediated cleavage of amyloid precursor protein. Science Translational Medicine, 2021, 13(585): eabe6178.

[24] SANDERS O D, RAJAGOPAL L, RAJAGOPAL JA. The oxidatively damaged DNA and amyloid-β oligomer hypothesis of Alzheimer's disease. Free Radical Biology Medicine, 2022, 179: 403–412.

[25] HAMPEL H, HARDY J, BLENNOW K, et al. The amyloid-β pathway in alzheimer's Disease. Molecular Psychiatry, 2021, 26(10): 5481–5503.

[26] DORE K, CARRICO Z, ALFONSO S, et al. PSD-95 protects synapses from β-amyloid. Cell Reports, 2021, 35(9): 109194.

[27] WANG XJ, QI L, CHENG YF, et al. PINK1 overexpression prevents forskolin-induced tau hyperphosphorylation and oxidative stress in a rat model of Alzheimer's disease. Acta Pharmacologica Sinica, 2022, 43(8): 1916–1927.

[28] SHANAKI BAVARSAD M, SPINA S, OEHLER A, et al. Comprehensive mapping of synaptic vesicle protein 2A (SV2A) in health and neurodegenerative diseases: a comparative analysis with synaptophysin and ground truth for PET-imaging interpretation. Acta Neuropathologica, 2024, 148(1): 58.

[29] YU Y, CHEN R, MAO KY, et al. The role of glial cells in synaptic dysfunction: insights into Alzheimer's disease mechanisms. Aging and Disease, 2024, 15(2): 459–479.

[30] YE LX, WANG X, CAI CC, et al. FGF21 promotes functional recovery after hypoxic-ischemic brain injury in neonatal rats by activating the PI3K/Akt signaling pathway via FGFR1/β-klotho. Experimental Neurology, 2019, 317: 34–50.

[31] RAZANI E, POURBAGHERI-SIGAROODI A, SAFAROGHLI-AZAR A, et al. The PI3K/Akt signaling axis in Alzheimer's disease: a valuable target to stimulate or suppress? Cell Stress and Chaperones, 2021, 26(6): 871-887.

[32] WANG HL, LI QQ, SUN SY, et al. Neuroprotective effects of salidroside in a mouse model of Alzheimer's disease. Cellular and Molecular Neurobiology, 2020, 40(7): 1133–1142.

[33] POLLEN AA, BHADURI A, ANDREWS MG, et al. Establishing cerebral organoids as models of human-specific brain evolution. Cell, 2019, 176(4): 743–756.

[34] NEIS VB, MORETTI M, ROSA PB, et al. The involvement of PI3K/Akt/mTOR/GSK3β signaling pathways in the antidepressant-like effect of AZD6765. Pharmacology, Biochemistry, and Behavior, 2020, 198: 173020.

[35] ZHENG MC, LIU ZH, MANA LL, et al. Shenzhiling oral liquid protects the myelin sheath against Alzheimer's disease through the PI3K/Akt-mTOR pathway. Journal of Ethnopharmacology, 2021, 278: 114264.

[36] YANG CZ, WANG SH, ZHANG RH, et al. Neuroprotective effect of astragalin via activating PI3K/Akt-mTOR-mediated autophagy on APP/PS1 mice. Cell Death Discovery, 2023, 9(1): 15.

补肾填髓方通过 PI3K 信号通路调节阿尔茨海默病模型中的突触损伤

惠珊[a], 郑庆[a], 李宏丽[b], 朱乐枚[b], 吴蓓蓓[b], 梁力晖[a*], 杨静静[c*]

a. 湖南师范大学第一附属医院湖南省人民医院老年病科, 湖南 长沙 410005, 中国
b. 中南大学湘雅二医院代谢疾病国家临床医学研究中心中西医结合科, 湖南 长沙 410011, 中国
c. 中南大学湘雅医院老年疾病国家临床医学研究中心临床护理教研室, 湖南 长沙 410008, 中国

【摘要】目的 探讨补肾填髓方及其活性成分淫羊藿苷对阿尔茨海默病（AD）的治疗作用及其机制。**方法** （1）动物实验。本研究使用无特定病原体（SPF）级别的雄性 C57BL/6J 野生型（WT）小鼠和 APP/PS1 双转基因小鼠进行实验，将小鼠分为 WT 组（WT 小鼠，$n = 5$，每日给予蒸馏水）、APP/PS1 组（APP/PS1 双转基因小鼠，$n = 5$，每日给予蒸馏水）和 BSTSD 组 [APP/PS1 双转基因小鼠，$n = 5$，以 27 g/(kg·d) 的剂量给予 BSTSD 悬浮液治疗 90 天]。采用 Morris 水迷宫（MWM）评估认知功能。实验后收集海马组织，通过苏木精-伊红（HE）染色和透射电子显微镜（TEM）分析锥体细胞和突触形态。（2）细胞实验。将 HT-22 细胞分为对照组（未处理）、A$\beta_{25\text{-}35}$ 组（用 20 μmol/L A$\beta_{25\text{-}35}$ 处理 24 小时）、淫羊藿苷组（先用 20 μmol/L 淫羊藿苷预处理 60 分钟，然后用 20 μmol/L A$\beta_{25\text{-}35}$ 再处理 24 小时）以及淫羊藿苷+LY294002 组 [用 20 μmol/L 淫羊藿苷和 20 μmol/L LY294002，一种磷脂酰肌醇-3-激酶（PI3K）信号通路抑制剂，处理 60 分钟，然后暴露于 20 μmol/L A$\beta_{25\text{-}35}$ 24 小时]，并测量细胞活力。使用 Western blot 检测突触相关蛋白 [突触素（SYP）和突触后密度蛋白-95（PSD-95）] 和 PI3K 信号通路相关蛋白 [磷酸化（p）-PI3K/PI3K、p-蛋白激酶（Akt）/Akt 和 p-哺乳动物雷帕霉素靶蛋白（mTOR）/mTOR）] 的表达水平。**结果** （1）动物实验。与 APP/PS1 组相比，BSTSD 组显示出逃避潜伏期显著缩短（$P < 0.01$），越过原始平台的频率显著增加（$P < 0.01$）。形态学观察显示，BSTSD 治疗后海马 CA1 区锥体细胞排列更规则，核染色均匀，空泡样变化减少。TEM 显示，与 APP/PS1 组相比，BSTSD 治疗组的突触活动区长度增加（$P < 0.01$），突触间隙宽度减少（$P < 0.01$）。（2）细胞实验。淫羊藿苷在不超过 20 μmol/L 的浓度下对 HT-22 细胞无明显毒性（$P > 0.05$），并且能够缓解 A$\beta_{25\text{-}35}$ 诱导的细胞活力下降（$P < 0.01$）。Western blot 结果显示，与 A$\beta_{25\text{-}35}$ 组相比，淫羊藿苷组的 p-PI3K/PI3K、p-Akt/Akt 和 p-mTOR/mTOR 的比值显著增加（$P < 0.01$），而 SYP 和 PSD-95 的蛋白表达水平也增加（$P < 0.01$）。这些效果可被 LY294002 所阻断（$P < 0.01$）。**结论** 补肾填髓方和淫羊藿苷通过激活 PI3K/Akt/mTOR 通路，增强 AD 模型中的认知功能和突触完整性，为潜在的治疗策略提供了可能。

【关键词】阿尔茨海默病；突触；补肾填髓方；淫羊藿苷；磷脂酰肌醇 3 激酶（PI3K）